HHS Public Access

Author manuscript

*Arterioscler Thromb Vasc Biol*. Author manuscript; available in PMC 2024 June 01.

Published in final edited form as:

*Arterioscler Thromb Vasc Biol*. 2023 June ; 43(6): 971–978. doi:10.1161/ATVBAHA.122.318509.

# Klf4 is not required for smooth muscle cell phenotype modulation in Marfan syndrome aortic aneurysm

**Albert J. Pedroza, MD**[1], **Alex R. Dalal, MD**[1], **Rohan Shad, MD**[1], **Nobu Yokoyama, MD**[1], **Ken Nakamura, MD**[1], **Olivia Mitchel, BS**[1], **Casey Gilles, BS**[1], **William Hiesinger, MD**[1], **Michael P. Fischbein, MD PhD**[1]

[1]Department of Cardiothoracic Surgery, Stanford University School of Medicine. Stanford CA, USA

## Abstract

**Background:** Smooth muscle cell (SMC) phenotypic reprogramming toward a mixed synthetic-proteolytic state is a central feature of aortic root aneurysm in Marfan syndrome (MFS). Previous work identified *Klf4* as a potential mediator of SMC plasticity in MFS.

**Methods:** MFS ($Fbn1^{C1041G/+}$) mouse strains with an inducible vascular SMC fluorescent reporter ($MFS^{SMC}$) with or without SMC-specific deletion of *Klf4* exons 2–3 ($MFS^{SMC\text{-}Klf4\Delta}$) were generated. Simultaneous SMC tracing and *Klf4* loss-of-function (*Klf4Δ* mice) was induced at 6 weeks of age. Aneurysm growth was assessed via serial echocardiography (4–24 weeks). 24-week-old mice were assessed via histology, RNA *in situ* hybridization, and aortic single-cell RNA sequencing (scRNAseq).

**Results:** MFS mice demonstrated progressive aortic root dilatation compared to control ($WT^{SMC}$) mice regardless of *Klf4* genotype ($p<0.001$) but there was no difference in aneurysm growth in $MFS^{SMC\text{-}Klf4\Delta}$ *vs.* $MFS^{SMC}$ ($p=0.884$). Efficient SMC *Klf4* deletion was confirmed via lineage-stratified genotyping, RNA *in-situ* hybridization, and immunohistochemistry. scRNAseq of traced SMCs revealed a highly similar pattern of phenotype modulation marked by loss of contractile markers (*e.g., Myh11, Cnn1*) and heightened expression of matrix genes (*e.g., Col1a1, Fn1*) between *Klf4* genotypes. Pseudotemporal quantitation of SMC dedifferentiation confirmed that *Klf4* deletion did not alter the global extent of phenotype modulation, but reduced expression of 23 genes during this phenotype transition in $MFS^{SMC\text{-}Klf4\Delta}$ mice, including multiple chondrogenic genes expressed by only the most severely dedifferentiated SMCs (*e.g., Cytl1, Tnfrsf11b*).

**Conclusions:** *Klf4* is not required to initiate SMC phenotype modulation in MFS aneurysm but may exert regulatory control over chondrogenic genes expressed in highly dedifferentiated SMCs.

## Graphical Abstract

Corresponding Author: Michael P. Fischbein, M.D. Ph.D., Associate Professor, Stanford University Department of Cardiothoracic Surgery. 300 Pasteur Dr, Falk CVRB, Stanford, CA 94305. (650) 721-2552, mfischbe@stanford.edu.

**Disclosures:** None

Supplementary Material:
- Supplemental Figure S1–S3
- Major Resources Table

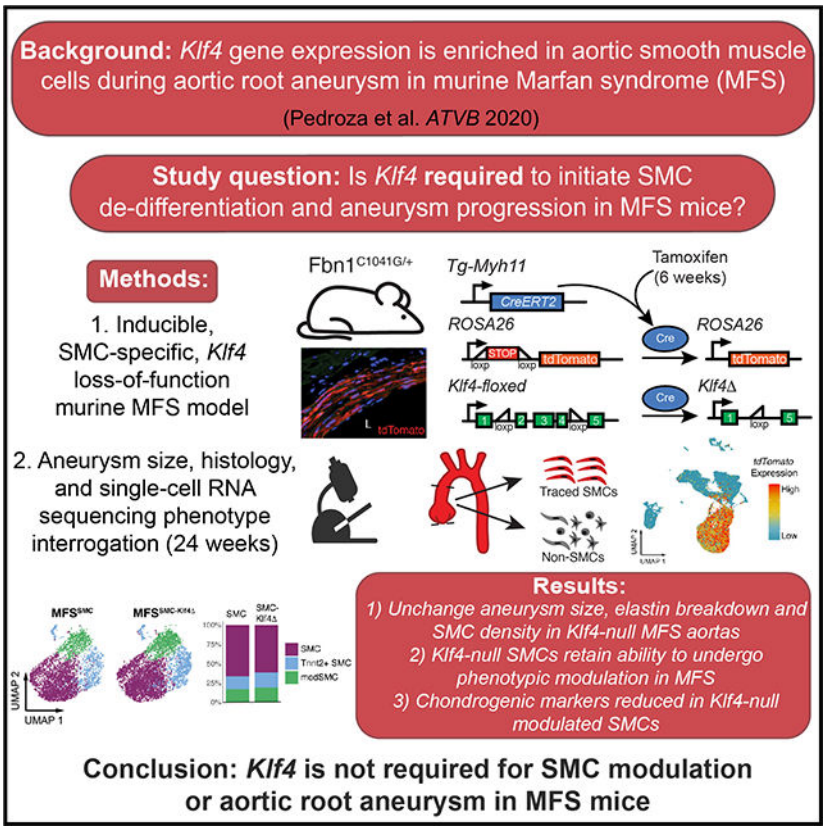


## Introduction

Smooth muscle cell phenotypic reprogramming toward a mixed synthetic-proteolytic state is a core feature of aortic root aneurysm progression in Marfan syndrome (MFS)[1,2]. This process promotes expression of central mediators of thoracic aortic aneurysm pathology including fibrillar collagens, matrix metalloproteinases and transforming growth factor-beta (TGF-β) ligands and is spatiotemporally restricted to the dilated proximal aorta (root and ascending) in *Fbn1*$^{C1041G/+}$ (MFS) mice[3]. While these associations suggest a critical role for SMC phenotype dysregulation, it remains unclear to what extent this process either contributes to aneurysm progression or potentiates a stabilizing effect through extracellular matrix (ECM) secretion and prevention of aortic rupture. Systematic identification and inhibition of transcription factors with central regulatory functions promoting phenotype transition is a critical aim toward achieving a clear understanding of the role SMC phenotypic plasticity plays in MFS aneurysm.

In a previous report, we identified kruppel-like factor 4 (*Klf4*) mRNA overexpression specifically in the aneurysm-associated 'modulated' SMC phenotype in MFS mice compared to healthy controls.[3] In this model, enriched *Klf4* expression correlated with concerted reduction of contractile gene expression and adoption of the synthetic phenotype in the aortic root, suggesting a role for this powerful regulatory gene in directing SMC phenotype in thoracic aortic aneurysm. *Klf4* has garnered broad appeal as a potential master regulator and therapeutic target in various vascular diseases[4]. Indeed, targeted SMC *Klf4*

knockout induced disease-ameliorating effects in advanced atherosclerotic lesions[5] and a degenerative atherosclerotic thoracic aortic aneurysm model[6]. Here, to test the hypothesis that *Klf4* contributes to the SMC phenotype modulatory process in MFS, we generated an analogous targeted SMC *Klf4* knockout MFS mouse strain and profiled the tissue and cellular phenotypes in advanced aortic root aneurysm.

## Methods

### Data Availability

Single cell RNA sequencing data (raw FASTQ and aligned data) have been made publicly available at the gene expression omnibus (GEO) repository under accession GSE206227.

### Statistical Analysis

Data were not prospectively analyzed for normality or equal variance. Statistical methods (linear mixed model for repeated measures and non-parametric testing for differential expression testing) were pre-specified. Longitudinal transthoracic echocardiography data (repeated measures on animal cohort) was analyzed via mixed effects linear model using the *lme4* and *lmerTest* packages in R. We examined the main and interaction effects of genotype (with littermate control as the reference) and time with a random effect for each replicate with aortic root diameter as the outcome. Pairwise comparisons were made using the *emmeans* package.

Differential expression testing within the single-cell RNA sequencing data, comprised pairwise Wilcoxon rank-sum testing for all cells within denoted clusters. P values were adjusted for multiple comparisons using the Bonferroni method and adjusted p values $<0.05$ were considered significant. For histologic analyses, nonparametric (Kruskal-Wallis) testing was first used to assess for significant differences between groups, followed by Dunn's multiple comparisons test for individual pairwise tests. Adjusted p values $<0.05$ were considered statistically significant.

## Mouse Strains

All animal studies were prospectively approved by the Institutional Animal Care and Use Committee at Stanford. All mouse strains were maintained on the C57BL/6J background. To generate smooth muscle lineage-traced MFS mice, we crossed $Fbn1^{C1041G/+}$ Marfan mice (strain #012885, The Jackson Laboratory) with a well-characterized tamoxifen-inducible *Cre* recombinase driven by the *Myh11* promoter ($Tg^{Myh11\text{-}CreERT2}$; strain #019079, The Jackson Laboratory)[7]. All male $Fbn1^{C1041G/+}$ progeny from these crosses carry the $Tg^{Myh11\text{-}CreERT2}$ transgene due to insertion on the Y chromosome. These males were crossed with floxed fluorescent reporter knock-in mice (B6.Cg-$Gt(ROSA)26Sor^{tm9(CAG\text{-}tdTomato)Hze}$/J, "$Rosa^{tdT/tdT}$"; strain #007909, The Jackson Laboratory)[8] to generate experimental mice. To generate conditional SMC-specific *Klf4* null mice, these breeding animals were iteratively crossed with mice carrying *loxP* sites flanking exons 2 and 4 of the *Klf4* gene ($Klf4^{loxP}$, MMRRC stock #029877-MU)[9] to generate homozygous floxed *Klf4* breeding pairs. Each allele was genotyped using sequence-specific PCR primers (see Major Resources Table in Supplement). Paired Marfan ($Fbn1^{C1041G/+}$)

and littermate control (*Fbn1*$^{+/+}$) mice from the same breeding crosses were utilized for all experiments.

### Induction of SMC tracing and Klf4 knockout by Cre recombinase

To induce permanent fluorescent labeling and, in *Klf4Δ* mice, simultaneous *Klf4* loss-of-function in SMCs, male mice were treated with two doses of 0.2mg g$^{-1}$ tamoxifen (Sigma) via oral gavage. Doses were administered 48 hours apart.

### Transthoracic Echocardiography

Mice were anesthetized with 2–3% inhaled isoflurane triplicate end-diastolic aortic root measurements were taken in long axis with an MS700 70 MHz MicroScan transducer on the Vevo 2100 system (VisualSonics, Toronto, Canada) by a blinded technician. Mean aortic diameter measurements from three separate cine clips were taken at 4-week intervals for all animals in each genotype cohort.

**Aortic tissue dissociation and sorting—**Aortic root/ascending aortic tissue (including the aortic valve up to the mid ascending aorta) was dissected from 24-week-old mice following anesthetic induction and exsanguination. Tissues were multiply washed in ice cold Hank's Balanced Salt Solution (HBSS) to remove all blood. Aortic tissue from n=4 replicate animals was pooled to achieve sufficient cell counts for cell sorting. Tissues were finely minced and digested in enzymatic buffer containing 2U/mL Liberase TL (Sigma) and 2U/mL elastase (Worthington) in HBSS with agitation at 37°C for 75 minutes. Cell suspensions were then passed through a 70μM filter and centrifuged at 500g for 5 minutes. Supernatant was removed and cells were resuspended in fresh HBSS. Cell suspensions were then sorted to remove debris and separate traced SMCs (tdTomato positive) from non-SMC populations (no fluorescence).

### Single-Cell RNA sequencing

Fresh, sorted cell populations were counted and processed for single-cell RNA sequencing as described previously.[10] RNA libraries were sequenced in parallel on a NovaSeq 6000 S1 flow cell. Raw data was then processed as described previously[10] using a custom mouse genome containing the *tdTomato* gene. Datasets were analyzed in parallel using the *Seurat* package in R to perform QC, normalization, scaling, principal component analysis and unsupervised clustering. Pseudotemporal analysis was performed using a wrapper for the *Monocle3* package in R and projecting the resulting pseudotime scores onto the *Seurat* data object. Source code for these analyses is available upon request.

**Lineage-segregated *Klf4* gDNA PCR—**Following tamoxifen induced recombination, thoracic aortic tissue was dissected from n=3 MFS$^{SMC}$, and MFS$^{SMC\text{-}Klf4\Delta}$ mice. A small piece of whole aorta was processed for genomic DNA extraction using QuckExtract DNA Extraction buffer (Lucigen, Middleton WI). The remaining thoracic aorta was enzymatically digested to generate a single cell suspension as in scRNAseq experiment methods. $2\times10^4$ traced SMCs (tdTomato positive) were sorted directly into DNA extraction buffer using a Sony SH800 device. Genomic DNA was extracted according to supplier protocols and diluted 1:10. PCR was then performed (42 cycles) using a

common forward primer for *Klf4* exon 1 (5'CTGGGCCCCCACATTAATGAG3') and reverse primers for *Klf4* exon 2 (5'CGCTGACAGCCATGTCAGACT3') and intron 4 (5'CAGAGCCGTTCTGGCTGTTTT3') to enable amplification of wild-type (172 bp), floxed (296 bp) and null (425 bp) alleles[9]. PCR products were analyzed via gel electrophoresis with a 2% agarose gel.

### Tissue Processing and Histology

Mice were deeply anesthetized with isoflurane and sacrificed by cervical dislocation followed by whole body perfusion with 4% paraformaldehyde in PBS. The proximal aorta (root and ascending aorta) was excised *en bloc* with the left ventricular outflow tract. Tissues were incubated in 4% paraformaldehyde overnight then passed through a sucrose gradient and embedded in optimal cutting temperature (OCT) in short axis. Tissue blocks were sectioned at 10μM thickness for RNAscope and 5μM for histologic stains.

### Histologic stains and analysis

5 μM sections were dried, rehydrated in PBS, and stained for either (1) hematoxylin and eosin (H&E) stain using a Rapid-Chrome H&E frozen section staining kit (Epredia Shandon) or (2) EVG stain using an Elastin Stain kit (Abcam ab150667) according to supplier specifications. For quantification of SMC density, replicate representative high-power field images of fixed dimensions were assessed from individual aortic root sections. Nuclei within the tunica media layer were counted by a blinded observer. Elastin fragmentation analysis was similarly performed on replicate high-power field images of fixed dimensions by a blinded observer. Quantifications were normalized by dividing the number of elastin breaks in each image by the total number of elastic lamina within a given section.

### *RNA* in situ *hybridization*

Aortic tissue sections were briefly dried at room temperature, rehydrated in PBS, and prepared for RNA hybridization via on-slide fixation with 4% paraformaldehyde, dehydration in ethanol, heat-activated target retrieval and protease treatment according to the BaseScope protocol (ACD Bio, Newark, CA). Sections were then incubated with a custom, sequence-specific probe targeting the exon 2–3 junction of mature *Klf4* mRNA followed by serial amplification probes using the chromogenic red BaseScope procedure kit according to supplier specifications. Following chromogenic detection, sections were counterstained with 50% hematoxylin and coverslipped with Vectamount media (Vector Laboratories, Burlingame, CA). Mouse positive and negative control probes were used in parallel on serial sections on the same microscope slide.

## Results

To specifically determine whether *Klf4*-mediated gene regulation is necessary for SMC phenotype modulation in MFS aneurysm, we generated $Fbn1^{C1041G/+}$ (MFS) mouse strains with a tamoxifen-inducible vascular SMC fluorescent reporter ($MFS^{SMC}$) with or without SMC-specific *Klf4* loss-of-function ($MFS^{SMC\text{-}Klf4\Delta}$). Six-week-old mice were treated with tamoxifen to induce permanent SMC tracing and simultaneous deletion of *Klf4* exons

2–3 in *Klf4Δ* mice (Figure 1A). We studied only male mice due to the *Myh11-Cre* transgene presence on the Y chromosome, and healthy male littermate controls ($WT^{SMC}$) were used for comparisons on the same genetic background. To confirm efficient *Cre*-mediated recombination, we genotyped the *Klf4* locus in (i) homogenized whole aortic root tissue and (ii) sorted SMCs from two replicate pools of $MFS^{SMC\text{-}Klf4\Delta}$ mice (n=2 biologic replicates of n=3 pooled animals for each replicate to isolate sufficient cells via FACS). While whole $MFS^{SMC\text{-}Klf4\Delta}$ tissue showed mosaicism with both floxed and null (recombined) PCR products, lineage-traced SMCs demonstrated only null *Klf4* alleles, confirming efficient recombination in these cells (Figure 1B). Efficient SMC *Klf4* knockout was further confirmed via absent immunohistochemical staining for *Klf4* in the tunica media layer of $MFS^{SMC\text{-}Klf4\Delta}$ aortic root sections (Supplemental Figure 1).

Next, to determine whether *Klf4* loss in SMCs affects aneurysm growth, we performed serial echocardiography from 4–24 weeks. MFS mice demonstrated progressive aortic root dilation compared to $WT^{SMC}$ regardless of *Klf4* genotype, (Figure 1C) but we found no significant difference in root aneurysm growth between $MFS^{SMC}$ and $MFS^{SMC\text{-}Klf4\Delta}$ mice ($p=0.884$, n=8 male mice per group). Histologically, we observed qualitatively similar ECM deposition and elastic laminar disruption in MFS mice compared to controls regardless of *Klf4* genotype. We found no statistically significant difference in medial SMC density between genotypes (Figure 1D). Elastin fragmentation was quantitatively increased in MFS mice relative to controls, however there was no significant difference in fragmentation between $MFS^{SMC}$ and $MFS^{SMC\text{-}Klf4\Delta}$ mice (Figure 1E).

Having shown that *Klf4* loss does not materially influence MFS aneurysm growth or tissue morphology, we next interrogated whether *Klf4* deletion affected SMC phenotype modulation. We performed single-cell RNA sequencing (scRNAseq) on aortic root tissue from four pooled 24-week-old $MFS^{SMC}$ and $MFS^{SMC\text{-}Klf4\Delta}$ mice, generating separate libraries for traced SMC (tdTomato fluorescent) and non-SMC populations (Figure 2A). Specifically investigating the traced (*tdTomato* mRNA-expressing) SMC populations, unsupervised clustering identified three distinct SMC clusters (Figure 2B) including mature contractile SMCs, phenotypically modulated SMCs ('modSMCs') characterized by reduced contractile gene expression (*e.g., Myh11*) and enriched ECM synthetic genes (*e.g., Col1a1*). We also identified a third minor population of *Tnnt2*-expressing SMCs, an aortic root-specific SMC subtype with minimal participation in the phenotype modulation process in MFS mice.[10] We have previously characterized the coordinated gene expression pathways altered during progressive phenotypic derangement of modSMCs during MFS aneurysm growth, including the activation of *Klf4* in SMCs undergoing modulation[3]. Similarly, in the present (combined $MFS^{SMC}$ and $MFS^{SMC\text{-}Klf4\Delta}$) dataset, modSMCs were distinguished from SMCs by differential expression of 1,172 genes including enriched *Klf4* (average $\log_2$ fold-change 0.49, $p=3.2\times10^{-34}$, Figure 2C, complete gene set presented in Supplemental Table 1). As reported in our previous work, direct comparison of MFS and analogous littermate control scRNAseq data confirmed that MFS SMCs activate *Klf4* expression specifically in the modSMC subset (Supplemental Figure 2). Critically, although *Klf4* mRNA detection via scRNAseq was even more pronounced in $MFS^{SMC\text{-}Klf4\Delta}$ modSMCs relative to $MFS^{SMC}$,these reads mapped only to the residual null allele with no detectable reads in the intervening deleted exons in $MFS^{SMC\text{-}Klf4\Delta}$ mice (Supplemental Figure 3),

providing further confirmation of *Klf4* loss-of-function in these SMCs. Furthermore, RNA in-situ hybridization with a custom probe targeting exons 2–3 of *Klf4* mRNA identified sparse but detectable amplification in $MFS^{SMC}$ mouse tunica media and absent signal in $MFS^{SMC\text{-}Klf4\Delta}$ (Figure 2C).

Directly comparing the SMC subsets between $MFS^{SMC\text{-}Klf4\Delta}$ and $MFS^{SMC}$ disclosed similar proportions of modSMCs (16.2% *vs.* 18.6%, respectively), confirming comparable progression of SMC phenotype independent of *Klf4* status (Figure 2D). Although these data indicate that *Klf4* loss was insufficient to prevent SMC modulation, we hypothesized that it may affect the ultimate phenotypic identity of the modSMC cluster. Comparing the modSMC cluster between $MFS^{SMC\text{-}Klf4\Delta}$ and $MFS^{SMC}$ samples, we identified 33 differentially expressed genes (Supplemental Table 2), with 23 genes enriched in $MFS^{SMC}$ including multiple metallothioneins (*Mt1/Mt2*), CCAAT/enhancer binding proteins (*Cebpb, Cebpd*), and multiple chondrogenic markers (*Cytl1/Tnfrsf11b*). To map the expression of these genes during the continuous phenotypic spectrum of SMC-modSMC transition, we performed pseudotemporal cell ordering ('pseudotime') on these clusters. Pseudotime value distribution was highly similar between genotypes and was associated with the SMC de-differentiation (*e.g.*, reduced *Myh11,* enriched *Fn1*, Figure 2E). Mapping expression of representative genes with reduced expression in $MFS^{SMC\text{-}Klf4\Delta}$ mice (*e.g., Mt1, Cebpb, Tnfrsf11b, Cytl1*) showed that these genes are activated in the most advanced cells in the trajectory of phenotypic de-differentiation (*e.g.,* highest pseudotime values) with diminished expression in SMCs lacking *Klf4* (Figure 2F).

## Discussion:

Using a transgenic, targeted SMC *Klf4* deletion MFS model, we discern that *Klf4*-mediated transcriptional regulation is not required to initiate or propagate SMC phenotype modulation in MFS aortic aneurysm. Critically, our scRNAseq dataset confirmed that *Klf4* transcription is activated along the trajectory of SMC modulation in MFS, consistent with our prior work. While we identified greater *Klf4* mRNA reads in the $MFS^{SMC\text{-}Klf4\Delta}$ model, we confirmed that these reads reflect expression only of the null allele *in silico*, with no detectable expression of the deleted exons. We attribute this finding to a failed compensatory response in *Klf4*-null SMCs to activate *Klf4* expression during SMC modulation. Effective *Klf4* loss-of-function was further validated *in situ* using a targeted RNA *in situ* hybridization probe for the deleted exons. Finally, effective SMC-specific *Klf4* deletion was further supported with orthogonal DNA and protein techniques.

While the lack of overall aneurysm phenotypic alteration in this model contrasts with analogous *Klf4* loss-of-function studies in atherosclerosis[5] and degenerative aneurysms[6], fate-mapped SMCs in those models exhibited extreme phenotypic plasticity including overtly chondrogenic/osteogenic fates. While we previously reported some chondrogenic marker expression in the MFS modSMCs (e.g., *Cytl1, Tnfrsf11b*), particularly from SMCs of neural crest origin[10], we have not observed SMC transformation into the overtly cartilaginous or bony phenotype reported in these models. Furthermore, these models employ atherogenic diets defined by hypercholesterolemia, which is recognized to promote *Klf4* expression and phenotypic modulation in SMCs.[11] These critical distinctions may

provide further insight into the way *Klf4* directs aortic SMC phenotype *in vivo.* Alencar *et al.* reported starkly reduced *Col2a1/Cytl1*-expressing chondrogenic SMC derivatives at the most extreme pole of SMC de-differentiation following *Klf4* ablation in advanced atherosclerotic lesions[5]. Our scRNAseq data revealed that genes most substantially reduced in $MFS^{SMC\text{-}Klf4\Delta}$ modSMCs similarly represented the most extreme pole of MFS-specific modulation—a phenotype evidently far less de-differentiated than in advanced atherosclerosis. Taken together, we conclude that while *Klf4* may participate in the progressive SMC de-differentiation process in MFS, this transcription factor may principally affect genes expressed only at the end of the SMC modulation pathway. Consequently, we speculate that *Klf4* may operate too far along the MFS phenotypic modulation pathway to materially impact cell phenotype or, more importantly, aneurysm progression through targeted SMC *Klf4* loss.

This study was limited by analysis at a single time point corresponding to an advanced state of aneurysm progression. Interestingly, we recently employed single-cell epigenetic profiling of MFS aortic SMCs in moderate aneurysm (16 weeks old), identifying multiple candidate regulatory signals of earlier-stage SMC phenotype modulation[10]. This analysis did not identify enriched *Klf4* DNA motif accessibility in 16-week-old modSMCs, further supporting a more temporally limited role for *Klf4* as a late disease modifier. While these findings suggest that *Klf4* loss could impact further SMC dysregulation in late aneurysm progression, this would be of questionable value toward the goal of arresting aneurysm initiation at a clinically relevant stage. In this light, future endeavors to identify and inhibit regulatory signals in MFS must target key triggering events earlier in aneurysm pathogenesis.

## Supplementary Material

Refer to Web version on PubMed Central for supplementary material.

## Acknowledgments:

We thank the Stanford Genome Sequencing Service Center for assistance with single-cell RNA sequencing.

### Sources of Funding:

This work was supported by grants from National Institute of Health F32HL154681 (AJP), F32HL160058 (ARD), R01HL157949 (MPF), and from the American Heart Association #834986 (RS). The NovaSeq 6000 device used in this study was purchased using NIH grant S10OD025212 funds.

## Non-standard Abbreviations and Acronyms

| | |
|---|---|
| **MFS** | Marfan Syndrome |
| **TGF-β** | transforming growth factor-beta |
| **ECM** | extracellular matrix |
| **scRNAseq** | single cell RNA sequencing |

## References


1. Bunton TE, Biery NJ, Myers L, Gayraud B, Ramirez F, Dietz HC. Phenotypic alteration of vascular smooth muscle cells precedes elastolysis in a mouse model of Marfan syndrome. Circ Res 2001;88:37–43. doi:10.1161/01.res.88.1.37. [PubMed: 11139471]
2. Crosas-Molist E, Meirelles T, López-Luque J, et al. Vascular smooth muscle cell phenotypic changes in patients with Marfan syndrome. Arterioscler Thromb Vasc Biol 2015;35:960–972. doi:10.1161/ATVBAHA.114.304412. [PubMed: 25593132]
3. Pedroza AJ, Tashima Y, Shad R, Cheng P, Wirka R, Churovich S, Nakamura K, Yokoyama N, Cui JZ, Iosef C, Hiesinger W, Quertermous T, Fischbein MP. Single-Cell Transcriptomic Profiling of Vascular Smooth Muscle Cell Phenotype Modulation in Marfan Syndrome Aortic Aneurysm. Arterioscler Thromb Vasc Biol 2020;40:2195–2211. doi:10.1161/ATVBAHA.120.314670. [PubMed: 32698686]
4. Yap C, Mieremet A, de Vries CJM, Micha D, de Waard V. Six Shades of Vascular Smooth Muscle Cells Illuminated by KLF4 (Krüppel-Like Factor 4). Arterioscler Thromb Vasc Biol 2021;41:2693–2707. doi:10.1161/ATVBAHA.121.316600. [PubMed: 34470477]
5. Alencar GF, Owsiany KM, Karnewar S, et al. Stem Cell Pluripotency Genes Klf4 and Oct4 Regulate Complex SMC Phenotypic Changes Critical in Late-Stage Atherosclerotic Lesion Pathogenesis. Circulation 2020;142:2045–2059. doi:10.1161/CIRCULATIONAHA.120.046672. [PubMed: 32674599]
6. Chen P-Y, Qin L, Li G, et al. Smooth Muscle Cell Reprogramming in Aortic Aneurysms. Cell Stem Cell 2020;26:542–557.e11. doi:10.1016/j.stem.2020.02.013. [PubMed: 32243809]
7. Wirth A, Benyó Z, Lukasova M, Leutgeb B, Wettschureck N, Gorbey S, Orsy P, Horváth B, Maser-Gluth C, Greiner E, Lemmer B, Schütz G, Gutkind JS, Offermanns S. G12-G13-LARG-mediated signaling in vascular smooth muscle is required for salt-induced hypertension. Nat Med 2008;14:64–68. doi:10.1038/nm1666. [PubMed: 18084302]
8. Madisen L, Zwingman TA, Sunkin SM, Oh SW, Zariwala HA, Gu H, Ng LL, Palmiter RD, Hawrylycz MJ, Jones AR, Lein ES, Zeng H. A robust and high-throughput Cre reporting and characterization system for the whole mouse brain. Nat Neurosci 2010;13:133–140. doi:10.1038/nn.2467. [PubMed: 20023653]
9. Katz JP, Perreault N, Goldstein BG, Lee CS, Labosky PA, Yang VW, Kaestner KH. The zinc-finger transcription factor Klf4 is required for terminal differentiation of goblet cells in the colon. Dev Camb Engl 2002;129:2619–2628.
10. Pedroza AJ, Dalal AR, Shad R, Yokoyama N, Nakamura K, Cheng P, Wirka RC, Mitchel O, Baiocchi M, Hiesinger W, Quertermous T, Fischbein MP. Embryologic Origin Influences Smooth Muscle Cell Phenotypic Modulation Signatures in Murine Marfan Syndrome Aortic Aneurysm. Arterioscler Thromb Vasc Biol 2022:101161ATVBAHA122317381. doi:10.1161/ATVBAHA.122.317381.
11. Chattopadhyay A, Kwartler CS, Kaw K, Li Y, Kaw A, Chen J, LeMaire SA, Shen YH, Milewicz DM. Cholesterol-Induced Phenotypic Modulation of Smooth Muscle Cells to Macrophage/Fibroblast-like Cells Is Driven by an Unfolded Protein Response. Arterioscler Thromb Vasc Biol 2021;41:302–316. doi:10.1161/ATVBAHA.120.315164. [PubMed: 33028096]

**Highlights:**

- *Klf4* expression is not required to initiate smooth muscle cell phenotype modulation in Marfan syndrome aortic root aneurysm.
- *Klf4* may promote the acquisition of a chondrogenic phenotype in advanced stages of smooth muscle cell de-differentiation.
- Future efforts to alter the trajectory of smooth muscle cell behavior in aortic aneurysm should target regulatory genes activated early in the disease process.

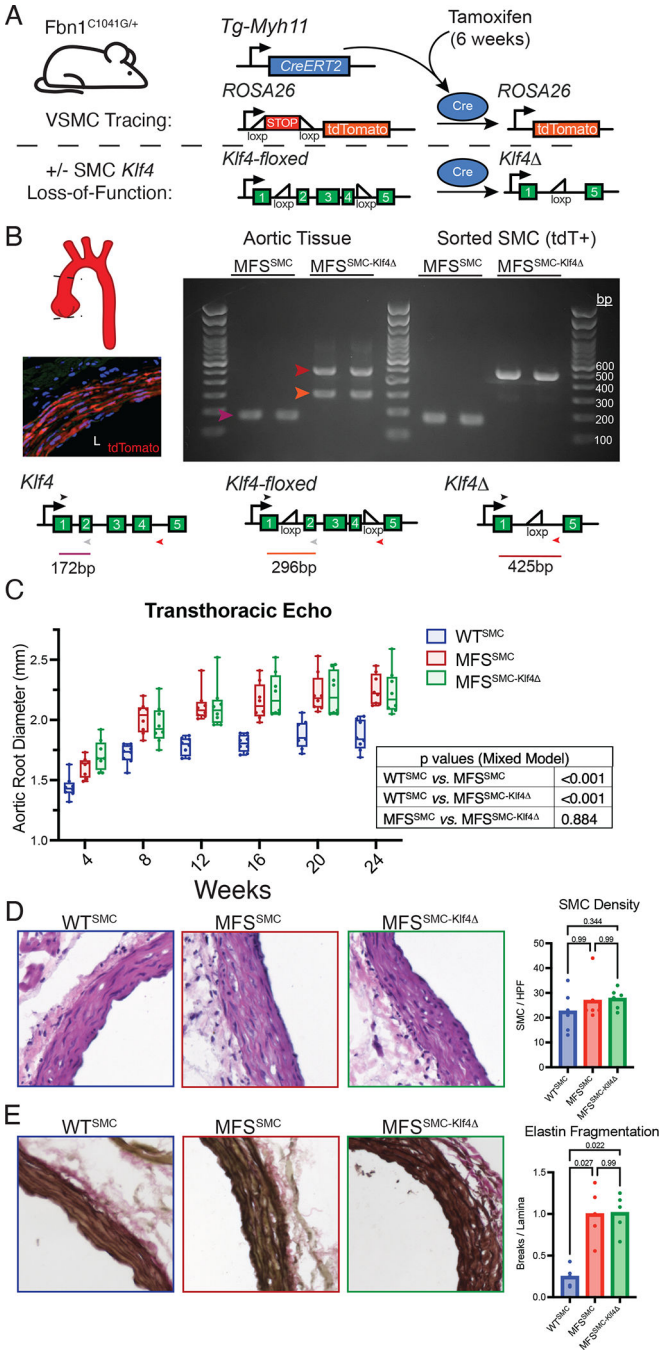


**Figure 1:**

Smooth muscle cell (SMC)-specific *Klf4* deletion in Marfan syndrome (MFS) mice does not affect aortic root aneurysm growth. **A** Experimental model. SMC fate-traced *Fbn1*$^{C1041G/+}$ MFS mice have *Myh11-CreERT2* transgene and inducible fluorescent reporter. Tamoxifen treatment induces excision of a stop cassette proximal to *tdTomato* gene within the constitutively expressed *Rosa26* locus. In *Klf4Δ* mice, homozygous floxed *Klf4* exons 2–4 enable loss-of-function with *CreERT2*-mediated excision. **B** Efficient recombination was confirmed via tdTomato fluorescence and lineage-stratified PCR. Genomic DNA from aortic

root whole tissue and positive sorted SMCs (*tdTomato* fluorescent) was amplified with primers within *Klf4* exon 1 (black arrowhead), exon 2 (reverse grey arrowhead), and intron 4 (reverse red arrowhead) were used to amplify wild-type *Klf4* (172bp), floxed (296bp), and null (recombined) alleles (425bp). **C** Transthoracic echo for repeated measures of n=8 male mice from each genotype. P values represent mixed effects linear model using random effect for each replicate. **D** Representative aortic root H&E stain and SMC density quantification in 24-week-old $WT^{SMC}$ control, $MFS^{SMC}$, and $MFS^{SMC\text{-}Klf4\Delta}$ mice demonstrates similar medial thickening and cellularity in MFS regardless of *Klf4* phenotype. (n=6 mice). **E** Representative EVG stains and quantification with similar aortic root elastin fragmentation and matrix disarray in MFS mice from both *Klf4* genotypes at 24 weeks.

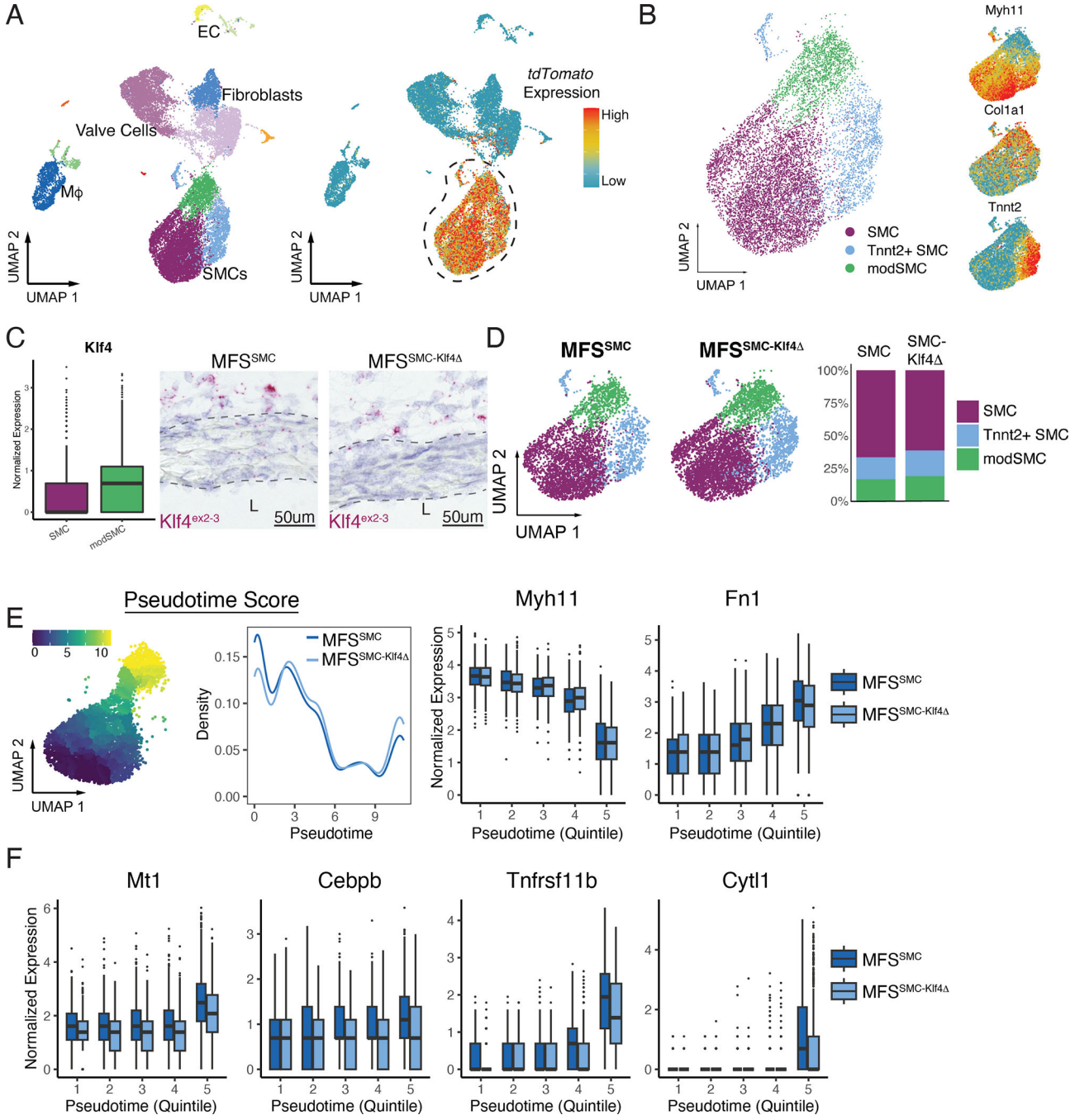


**Figure 2:**

*Klf4* loss in MFS aortic SMCs does not prevent phenotypic modulation during aneurysm development. **A** Complete scRNAseq dataset from both *Klf4* genotypes at 24 weeks. Left: unsupervised cell clustering including three SMC subsets. Right: *tdTomato* mRNA expression confirming SMC clusters. **B** SMC subtypes identified by clustering distinguished by heightened contractile gene expression ('SMC'), extracellular matrix component expression ('modSMC'), and cardiac troponin ('Tnnt2+ SMC'). **C** *Klf4* mRNA expression is heightened in modSMC cluster (left). Deleted *Klf4* exons are not amplifiable in

*MFS*$^{SMC\text{-}Klf4\Delta}$ mouse tunica media (right). **D** SMC clusters stratified by *Klf4* genotype showing similar ratios of quiescent ('SMC') and modulated ('modSMC') subsets. **E** Pseudotime scoring of SMC-modSMC phenotypic trajectory with score distributions stratified by *Klf4* genotype. Boxplots show gene expression median and interquartile range (line and box) throughout pseudotime binned into quintiles. Bottom row depicts differentially expressed genes reaching statistical significance in modSMC subset between *Klf4* genotypes.